Structure Dependence of Electron Spin Polarization in Zn−Porphyrin−Quinone Ensembles Oriented in a Liquid Crystal

Alexander Berg, Zohar Shuali, and Haim Levanon*

Department of Physical Chemistry, The Hebrew University of Jerusalem, Jerusalem 91904, Israel

Arno Wiehe† **and Harry Kurreck**

Institute of Organic Chemistry, Free University Berlin, Takustrasse 3, D-14195 Berlin, Germany

Received: May 21, 2001

Photoinduced intramolecular electron transfer was studied by time-resolved electron paramagnetic resonance spectroscopy in two photosynthetic model systems oriented in a nematic liquid crystal. The donor−acceptor assemblies consisted of differently substituted zinc porphyrins covalently linked to a quinone with different spacers, i.e., triptycyl and cyclohexylene. The orientation of the guest molecules with respect to the director of the liquid crystal was determined by line shape analysis of their triplet spectra and by molecular modeling. It is demonstrated that the polarized pattern of the radical pair spectrum is sensitive mainly to the spacer structure, but to some extent also to the peripheral substituents.

Introduction

Primary photosynthesis is typified by a subsequent series of electron transfer (ET) events in the reaction center, which produce long-lived charge-separated states with high quantum yield. These states, in turn, convert light energy to chemical potential to be utilized in the biochemical reactions.[1]

The complexity of the in vivo apparatus prompts the search for model systems, which can mimic the major features occurring in photosynthetic reaction centers. Although not yet fully understood, it is evident that the structure−function relationships between the participants of the ET chain and interactions with their environment make the photosynthetic apparatus unique.[2] In this context, a large number of supramolecular model systems embedded in isotropic and anisotropic matrixes have been studied to mimic the biological ET pathways.[3−5] In these systems the donor (D) and acceptor (A) are (1) linked together covalently via a spacer (*s*),[6−9] (2) linked by electrostatic forces,[10,11] and (3) base paired via hydrogen bonds.[12−14] The data obtained allow relating the rate and efficiency of the electron and energy transfer processes with structural factors, energetics (i.e., driving forces), temperature, and medium properties. As to the role of the microenvironment, it was demonstrated[3,15] that liquid crystals (LCs), due to their unique physical and chemical properties, are ideal solvents to attenuate ET rates into the submicrosecond time scale, thus allowing us to study electron spin dynamics by time-resolved EPR (TREPR) over a wide temperature range (∼100 deg) including ambient temperatures.

In this work we report on the TREPR study of photoinduced intramolecular electron transfer (IET) in two covalently linked DsA model systems oriented in the nematic LC (E-7): (1) {5-[2-(5,8,9,10-tetrahydro-6,7-dimethyl-5,8-dioxo-9,10-(*o*-benzeno)-anthracenyl)]-10,15,20-tritolylporphyrinato}zinc(II) (structure left) and (2) {5-[4(e)-(1,4-dioxocyclohexa-2,5-dien-2-yl)cyclohex-(e)-yl]-10,15,20-tris[3-(4-pentoxybiphenyl-4′-oxy)phenyl]-porphyrinato}zinc(II) (structure right) named ZnP-*t*Q and ZnP-*c*Q.

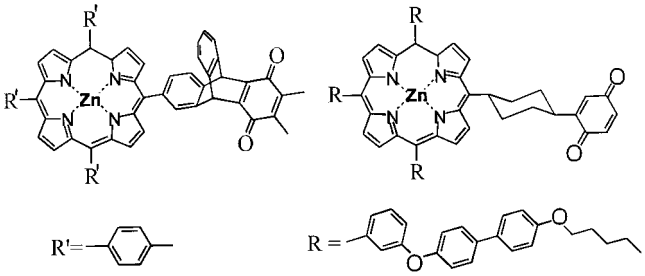

The light-driven processes occurring in these systems can be expressed by the set of reactions:

$$\mathrm{DsA} \xrightarrow{h\nu} {}^{1*}\mathrm{DsA} \xrightarrow{\mathrm{ISC}} {}^{3*}\mathrm{DsA} \xrightarrow{\mathrm{ET}} {}^{3}(\mathrm{D}^{\bullet+}\mathrm{s}\,\mathrm{A}^{\bullet-}) \leftrightarrow {}^{1}(\mathrm{D}^{\bullet+}\mathrm{sA}^{\bullet-}) \quad (1)$$

(ET)

where selective light excitation of the porphyrin moiety results in IET from the photoexcited porphyrin to the quinone to generate the radical pairs (RP).

The difference between two systems studied is that while the cyclohexylene spacer in ZnP-*c*Q allows some flexibility of the quinone with respect to the bridge and porphyrin plane,[16,17] such a degree of freedom due to pronounced steric restrictions is absent in ZnP-*t*Q. [18,19] Moreover, the long-chain substitution on the porphyrin periphery, which is collinear with the cyclohexylene bridge, enhances the spacer's fluctuations, thus affecting the polarization pattern of the RP formed. Within the time resolution of our experimental setup, we have not observed any evidence for singlet-initiated IET, as depicted by eq 1. Therefore, the different polarization patterns in the TREPR spectra of the RPs are discussed in terms of the relative mutual orientation of the donor and acceptor moieties.

† Present address: Institute of Physics, Humboldt University Berlin, Invalidenstrasse 110, 10115, Germany.

10.1021/jp0119227 CCC: $20.00
Published on Web 10/09/2001

Experimental Section

ZnP-*t*Q and ZnP-*c*Q were synthesized as described elsewhere.[19,20] Toluene (Baker analyzed, ACS reagent) was dried over a Na/K mirror and was kept under vacuum throughout sample preparation. Ethanol and dichloromethane (Aldrich, HPLC grade) were used without further purification. For the studying of the systems in isotropic solvents, the samples of ZnP-*t*Q were prepared in toluene and in ethanol, and the samples of ZnP-*c*Q were prepared in toluene and in 1:1 ethanol−dichloromethane mixture, which was used because of the low solubility of the compound in ethanol. The LC (E-7, Merck Ltd.) used is characterized by the positive diamagnetic susceptibility, $\Delta\chi$, and exhibits the following phase transitions as a function of temperature:

$$\text{E7:}\quad \text{crystalline} \xleftrightarrow{210\ \text{K}} \text{soft crystal} \xleftrightarrow{263\ \text{K}} \text{nematic} \xleftrightarrow{333\ \text{K}} \text{isotropic}$$

Since the orientation of the LC director, **L**, with respect to the magnetic field, **B**, is dictated by the sign of $\Delta\chi$,[22] the default orientation in the nematic phase of E-7 is **L**||**B**.

Optical absorption spectra were taken on a Hewlett-Packard Vectra 5 spectrometer. The EPR samples (concentration $\sim 5 \times 10^{-4}$ M) were prepared in 4 mm o.d. Pyrex tubes under vacuum. The samples were excited at 560 nm (Q-band absorption range of porphyrin) by dye laser (Continuum TSL-60) flashes (2 mJ/pulse, 20 Hz repetition rate, ~10 ns pulse duration) pumped by the second harmonic of an Nd:YAG laser (Continuum 661-20). TREPR measurements were carried out on a Bruker ESP-380 with a variable-temperature unit Bruker ER411 VT in direct detection mode (response time of ~250 ns). The magnetic field was calibrated using 1,1-diphenyl-2-picrylhydrazyl ($g = 2.0036$). A detailed description of experimental setup is given elsewhere.[23,24] The analysis of the TREPR spectra and the time profiles of the magnetization, $My(t)$ are performed as described elsewhere.[6,7] The molecular modeling was carried out using the computer program HyperChem-4, which provides the minimum energy structure of the molecules. It should be noticed that these calculations do not take into account the LC environment, and thus some deviations are expected.

Results and Discussion

The line shape of a triplet EPR spectrum of a chromophore embedded in a LC is dictated by the molecular alignment with respect to the external magnetic field, **B** and the director, **L**.[25] The amplitude of the resulting signal is proportional to the corresponding magnetization component along a molecular axis and the projection of that component on **B** (or **L**).[7,22] The sign of the spin polarization is determined by the population difference between the two triplet levels, where EPR transitions occur.

Photoexcitation of frozen solutions of ZnP-*t*Q and ZnP-*c*Q in isotropic solvents as well as in the crystalline phase of E-7 gives rise to triplet-polarized spectra with the magnetic and spin dynamic parameters that are typical of ^{3*}ZnTPP (Table 1).[26] Therefore, we assume that in the present porphyrins as in ZnTPP, **L** lies along the opposite nitrogens in the porphyrin molecular *X*, *Y* plane and the out-of-plane *Z*-axis is the active state.[26,27] At freezing temperatures, in both the anisotropic (LC) and isotropic (toluene, ethanol, and ethanol−dichloromethane) media practically identical triplet spectra were observed and attributed to the triplet donor in ZnP-*t*Q and ZnP-*c*Q. This finding can be explained by a strong dependence of the ET rate constant on the solvent reorganization energy λ, viscosity, and dielectric relaxation time.[28,29] In the frozen media, where the motion of the solvent molecules is restricted, destabilization of the charge-separated state is increased by the value of λ. Thus, as a result, both RP states lie above the precursor triplet state and possibly above the singlet state, and uphill ET does not occur.

TABLE 1: Magnetic and Kinetic Parameters of the Photoexcited Triplets and Radical Pairs[a]

compound	$\lvert D\rvert$ (mT)	$\lvert E\rvert$ (mT)	T_1 (s)	T_2 (s)
^{3}ZnTPP	31.9	10.5	0.4×10^{-6}	1.2×10^{-7}
^{3}ZnP-*t*Q	31.0	9.0	4.3×10^{-6}	4×10^{-7}
^{3}(ZnP$^{\cdot+}$*t*Q$^{\cdot-}$)	2.6	0.2	6.6×10^{-6}	1×10^{-6}
^{3}ZnP-*c*Q	34.5	8.0	2.4×10^{-6}	4.7×10^{-7}
^{3}(ZnP$^{\cdot+}$*c*Q$^{\cdot-}$)	6.5/3.8	0.5/0.2	$3.7/5.5 \times 10^{-6}$	$8.3/7.4 \times 10^{-7}$

[a] Uncertainty: ±10%; all parameters of the ^{3}(ZnP$^{\cdot+}$*c*Q$^{\cdot-}$) spectrum are presented as the respective values for the conformer signals corresponding to outermost/innermost lines, respectively. The parameters of ^{3}ZnTPP are taken from ref 23.

Upon a temperature increase, no indication of IET is noticed with isotropic solvents (probably due to the fast ET rates, beyond TREPR detection time). However, when LCs are employed, increasing the temperature into the fluid nematic phase allows the triplet observation and subsequent IET. (All the experiments in the nematic phase of the LC were performed only for the case where **L**||**B** because the perpendicular orientation in the fluid phase is not observed since the director aligns itself along the external magnetic field.)

ZnP-*t*Q. Figure 1A−C depicts the time evolution of the TREPR spectra of ^{3*}ZnP-*t*Q in E-7 at 270 K (nematic phase). Early in time, only a broad signal is observed (Figure 1A), while later in time, a narrow derivative-like signal with an absorption/emission (a,e) phase pattern is superimposed on the broad spectrum (Figure 1B). The broad signal is ascribed to the lowest triplet state of ZnP moiety (see above). The *g*-value (~2.0033) of the narrow signal, which is presented in an expanded form in Figure 1C is in good agreement with the arithmetic mean of that of ZnP$^{\bullet+}$ ($g \sim 2.0025$)[30] and Q$^{\bullet-}$ ($g \sim 2.0047$).[31] The analysis of the magnetization profiles of these two signals demonstrates that the rise time of the narrow signal coincides with the broad signal decay (Figure 2A). On the basis of these findings, we attribute this narrow signal to a RP formed as result of the photoinduced IET from porphyrin to the quinone. The kinetic and magnetic parameters of this signal (Table 1) allowed us to assign it to the triplet radical pair ^{3}(ZnP$^{\bullet+}$-*t*Q$^{\bullet-}$) with a triplet genesis.

We explain the polarization pattern a,e of this signal by the polarization transfer from the porphyrin triplet state to the RP. In ^{3*}ZnTPP the zero-field *z* level is selectively populated via ISC and the corresponding *Z*-axis is perpendicular to the porphyrin plane.[26] As was shown in detail in previous studies of similar systems,[6,7] and as computer modeling predicts, the dipolar axis z' of ^{3}RP coincides with **L** and lies along the Zn−porphyrin−quinone connecting line, which is in the porphyrin plane. In our case the angle between *Z* and z' is ~78° (Figure 3A). Thus, the out-of-plane *Z*-axis polarization of the porphyrin is transferred mainly to the x' (or the equivalent, y') axis and only partially to the z' axis of the triplet RP,[6,7] giving rise to a two-line spectrum with the a,e polarization pattern (Figure 1C). Considering the inter-radical distance (center-to-center) in the RP of ~10.7 Å (calculated using HyperChem), or $r \sim 10$ Å as determined by Corey−Pauling−Koltun molecular models,[32] we have estimated the ZFS parameter *D*, which should be negative[33] by the point dipole approximation method. From the relation $\lvert D\rvert = {}^3/_4[(g\beta)^2/r^3]$, with a *g* factor of ~2.0033, the Bohr

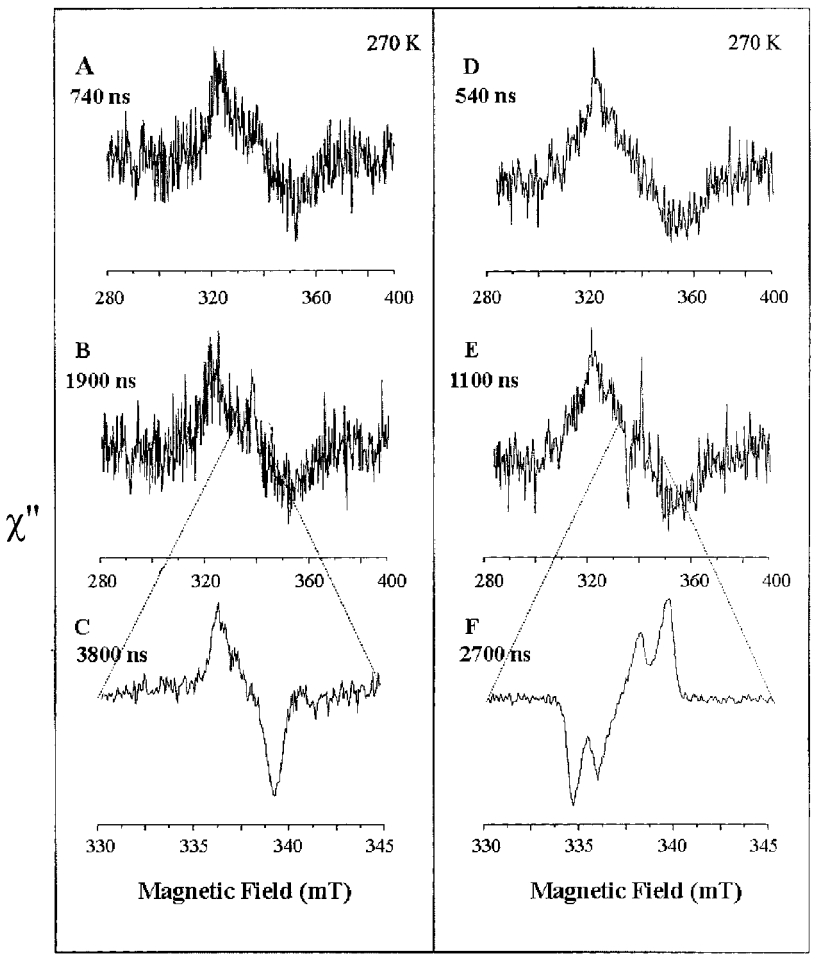

Figure 1. TREPR spectra (time evolution) of ZnP-*t*Q (A, B, and C) and ZnP-*c*Q (D, E, and F), in E-7 at 270 K. C and F: expanded TREPR spectra of ^{3}(ZnP$^{\bullet+}$-*t*Q$^{\bullet+}$) and ^{3}(ZnP$^{\bullet+}$-*c*Q$^{\bullet-}$) taken at 3800 and 2700 ns after the laser pulse, when the corresponding broad signals were completely decayed. Microwave power: 57 mW.

magneton β, r (in Å), and D (in Gauss), a value of $|D| \sim 2.2$ mT (2.7 mT for $r \sim 10$ Å) is obtained, which is in a good agreement with the value of $|D| = 2.6$ mT obtained from the line shape analysis of the triplet RP spectra. The above analysis assumes that the spin polarization of the RP is acquired by polarization transfer only. It is a reasonable assumption since the aromatic nature of the spacer and center-to-center separation of ~10 Å results in a large value (comparable with the Zeeman interaction) of exchange integral J, [34−36] which practically excludes the possibilities of singlet−triplet mixings in the RP.[37] Thus, transitions within the three triplet sublevels of ^{3}RP will dominate the EPR spectrum (Figure 4B).

ZnP-*c*Q. Figure 1D−F shows the time evolution of the TREPR spectrum of ^{3*}ZnP-*c*Q in the nematic phase of E-7 (270 K). In the early time window, the broad spin-polarized spectrum is observed (Figure 1D), which is practically the same as that of ^{3*}ZnP-*t*Q (Table 1), and is assigned to the lowest triplet state of ZnP. At later times, an additional narrow four-line polarized spectrum appears (e,e,a,a, and $g \sim 2.0035$) (Figure 1E,F). The analysis of the corresponding kinetic traces shows that the rise time of the narrow signal coincides with the decay time of the broad one (Figure 2B). On the basis of these findings and with similar arguments in calculating the g-factor as for ^{3}(ZnP$^{\bullet+}$-*t*Q$^{\bullet-}$), we attribute the narrow signal to the triplet spectrum of the radical pair ^{3}(ZnP$^{\bullet+}$-*c*Q$^{\bullet-}$), which is generated via light-driven IET from the porphyrin triplet to the quinone.

Comparing the RP signals in both systems (Figure 1C,F) shows that their line shapes are completely different: in the case of the ^{3}(ZnP$^{\bullet+}$-*t*Q$^{\bullet-}$) the spectrum consists of two lines with a,e polarization pattern (Figure 1C), whereas for the ^{3}(ZnP$^{\bullet-}$-*c*Q$^{\bullet-}$) a four-line spectrum with an e,e,a,a polarization pattern is observed (Figure 1F). We interpret these differences, observed in an identical environment under the same conditions, by structural peculiarities of the spacers in ZnP-*t*Q and ZnP-*c*Q, and to a lesser extent by the peripheral substituents. It is confirmed by the fact that a four-line spectrum with the same polarization pattern but less resolved components and different time evolution behavior was observed in plain ZnTPP linked to the quinone via cyclohexylene spacer.[6] The changes in the spacer structure result in different mutual donor−acceptor orientations and different possibilities of the quinone rotation with respect to the porphyrin plane, which, in turn, strongly affect the population of the RP triplet sublevels and S ↔ T mixing probability. [7,16]

As was stated above, the polarization patterns in the RP spectra originate from the polarization transfer between the two coordinate systems, X, Y, Z and x', y', z', corresponding to the porphyrin and RP, respectively. Molecular modeling combined with computer simulations shows that the z'-axis, which lies along the ZnP-*c*Q connecting line, deviates from the XY-plane by an angle of ~10° and from the director, **L**, by an angle of ~40° (Figure 3B). As a consequence, the porphyrin Z-axis should have components on both z' and x' (or y') axes of the RP.[6,7] More specifically, it was demonstrated that for the porphyrin−quinone ensemble bound via a rigid spacer (like ZnP-*t*Q), the most probable polarization transfer will occur

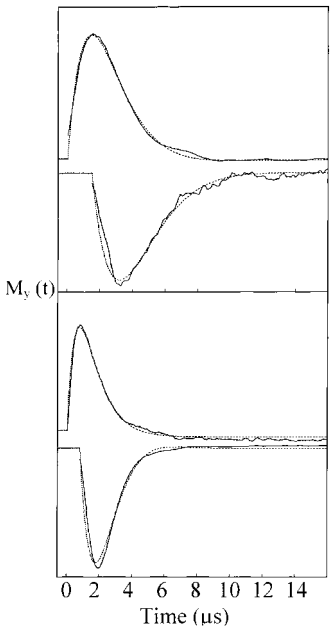

Figure 2. Magnetization, $M_y(t)$, traces of photoexcited ZnP-*t*Q (A) and ZnP-*c*Q (B) at 270 K in E-7. A: The upper trace is that of the ^{3}ZnP-*t*Q (taken at the low field of the absorption line), and the lower trace is that of the ^{3}(ZnP$^{\bullet+}$-*t*Q$^{\bullet-}$) (taken at the low field absorption line and inverted). B: The upper trace is that of the ^{3} ZnP-*c*Q (taken at the low field of the absorption line), and the lower trace is that of the ^{3}(ZnP$^{\bullet+}$-*c*Q$^{\bullet-}$) (taken at the low field emission outermost line). The solid lines superimposed on the experimental curves are best-fit computer simulations, for which results are given in Table 1. The kinetic trace of the innermost emission line exhibits the same shape, but with a noticeably longer decay.

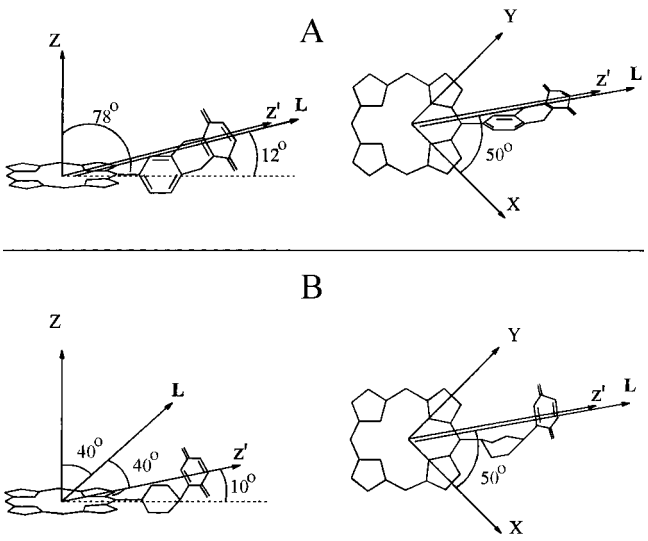

Figure 3. Side (left)- and front (right)- views of the calculated (HyperChem) minimum energy structures of ZnP-*t*Q (A) and ZnP-*c*Q, (B). X, Y, Z, and *x*′, *y*′, *z*′ are porphyrin and the RP molecular axes, respectively; **L** is the LC director.

mainly from the spin-active *Z*-axis to *x*′ (or *y*′).[6] Indeed, the rigid configuration of ZnP-*t*Q does not allow fluctuations of *z*′ with respect to *Z* to change this situation. [18] However, the flexibility of the cyclohexylene bridge and the quinone attached to it in the case of ZnP-*c*Q may account for the experimental spectral line shape and the polarization pattern. At relatively high temperature (270 K), the fluctuations of the dipolar axis *z*′ significantly increase the angle between *z*′ and the out-of-plane *Z* axis of porphyrin. Thus, in this case, this will result in the increase of the polarization transfer to *z*′. This situation is

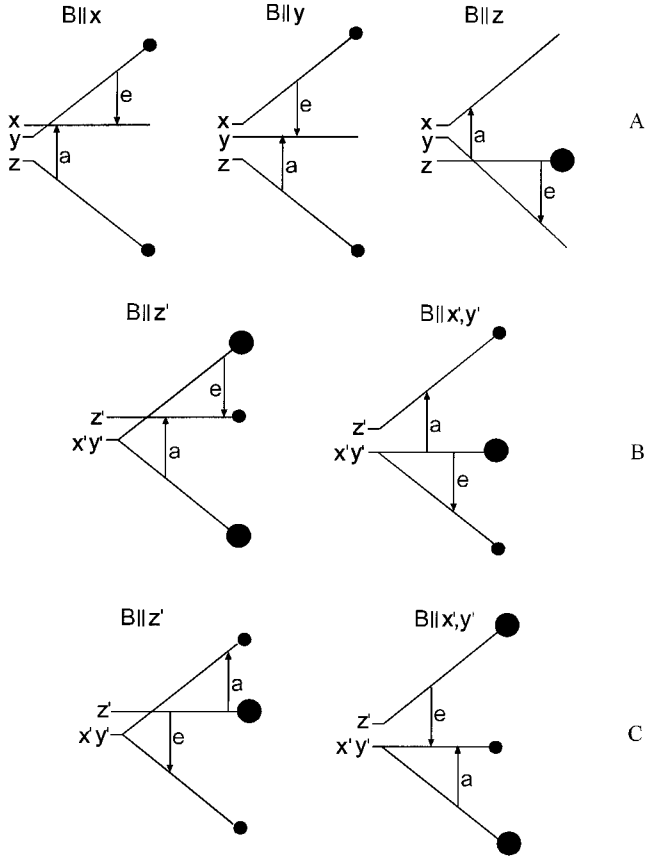

Figure 4. Energy level diagram of the triplet sublevels and EPR transitions: (A) ^{3}ZnP; (B) ^{3}(ZnP$^{\bullet+}$-*t*Q$^{\bullet-}$); (C) ^{3}(ZnP$^{\bullet+}$-*c*Q$^{\bullet-}$).

depicted in Figure 4C, accounting for the observed e,e,a,a polarization pattern. The large value of the exchange coupling found in a similar system ($|J|$ = 137.0 mT)[37] significantly reduces the S ↔ T mixing probability in the RP. Therefore, the TREPR spectrum of ^{3}RP is the result of transitions occurring only within the triplet manifold (Figure 4C).

As to the origin of the four-line spectrum, computer simulation of the spectrum shown in Figure 1F could be accomplished only by assuming the existence of two species with different center-to-center distances from which the first is associated with the outermost lines and the second one with the inner ones. The analysis of the kinetic traces of these signals shows that while they have practically the same rise times, the decay time of the former signal is noticeably slower than that of the latter one (see Table 1). We assign these species to triplet RPs formed in different conformers of ZnP-*c*Q, which differ from each other probably by conformation of the cyclohexylene bridge as a result of twist type geometry, which adopts this spacer in similar systems in isotropic solvents and LCs.[16,38−40] The center-to-center distances, i.e., ∼7.5 and ∼8.9 Å, were calculated via point dipole approximation, resulting in *D* parameters presented in Table 1. These values are in fairly good agreement with ∼9.8 Å obtained from HyperChem computer modeling for the minimum energy structure of the ensemble. It should be noticed here that a similar polarization pattern of the RP signal with the same kinetic behavior was found in the triad of the Zn porphyrin covalently linked to two quinones, i.e., ZnP−Q_1−Q_2.[17] The signal was assigned to a superposition of the spectra of two RPs, which were formed by photoinduced IET from porphyrin to the adjacent and far quinones, respectively. The formation of two, "folded" and "stretched" ET active conformers were also observed in the butylene-linked zinc porphyrin−quinone ensembles embedded in a LC.[39]

Conclusion

To summarize, we have demonstrated that in two DsA systems with modified spacers the electron spin polarization effects accompanied by photoinduced IET are strongly affected by the changes in donor−acceptor mutual orientation and, to some extent, by peripheral substituents of the donor.

Acknowledgment. The Farkas Center is supported by the Bundenministerium für Forschung and Technologie and the Minerva Geselschaft für die Forschung GMBH. The research described herein was supported by the Forschungszentrum Juelich GMBH (KFA), U.S.-Israel BSF and by the Volkswagen Stiftung (Schwerpunktprogramm Electronentransfer, Kurreck/Röder I/72381, Möbius/Levanon I/73145). We are grateful to Mr. A. Blank for providing us with the computer program for spectra simulations. We thank Dr. J. von Gersdorff for a generous gift of compound ZnP-*c*Q. This work was supported by the Deutsche Forschungsgemeinschaft (337 and Normalverfahren). H.K. thanks the Fonds der Chemischen Industrie for financial support.

References and Notes

(1) Sundström, V. *Prog. Quantum Electron.* **2000**, *24*, 187.
(2) Bixon, M.; Fajer, J.; Feher, G.; Freed, J. H.; Gamliel, D.; Hoff, A. J.; Levanon, H.; Möbius, K.; Nechushtai, R.; Norris, J. R.; Scherz, A.; Sessler, J. L.; Stehlik, D. *Isr. J. Chem.* **1992**, *32*, 369.
(3) Levanon, H.; Möbius, K. *Annu. Rev. Biophys. Biomol. Struct.* **1997**, *26*, 495.
(4) Gust, D.; Moore, T. A.; Moore, A. L. *Pure Appl. Chem*. **1998**, *70*, 2189.
(5) Tsue, H.; Imahori, H.; Kaneda, T.; Tanaka, Y.; Okada, T.; Tamaki, K.; Sakata, Y. *J. Am. Chem. Soc.* **2000**, *122*, 2279.
(6) Hasharoni, K.; Levanon, H.; von Gersdorff, J.; Kurreck, H.; Möbius, K. *J. Chem. Phys.* **1993**, *98*, 2916.
(7) Hasharoni, K.; Levanon, H.; Gätschmann, J.; Schubert, H.; Kurreck, H.; Möbius, K. *J. Phys. Chem.* **1995**, *99*, 7514.
(8) Elger, G.; Fuhs, M.; Muller, P.; von Gersdorff, J.; Wiehe, A.; Kurreck, H.; Möbius, K. *Mol. Phys.* **1998**, *95*, 1309.
(9) Korth, O.; Wiehe, A.; Kurreck, H.; Roder, B. *Chem. Phys*. **1999**, *246*, 363.
(10) Hugerat, M.; van der Est, A.; Ojadi, E.; Biczok, L.; Linschitz, H.; Levanon, H.; Stehlik, D. *J. Phys. Chem.* **1996**, *100*, 495.
(11) Berg, A.; Rachamim, M.; Galili, T.; Levanon, H. *J. Phys. Chem.* **1996**, *100*, 8791.
(12) Berman, A.; Izraeli, E. S.; Levanon, H.; Wang, B.; Sessler, J. L. *J. Am. Chem. Soc.* **1995**, *117*, 8252.
(13) Asano-Someda, M.; Levanon, H.; Sessler, J. L.; Wang, R. *Mol. Phys*. **1998**, *95*, 935.
(14) Berg, A.; Shuali, Z.; Asano-Someda, M.; Levanon, H.; Fuhs, M.; Möbius, K.; Wang, R.; Sessler, J. L. *J. Am. Chem. Soc*. **1999**, *121*, 7433.
(15) Levanon, H.; Hasharoni, K. *Prog. React. Kinet*. **1995**, *20*, 309.
(16) Poupko, R.; Luz, Z. *J. Chem. Phys*. **1981**, *75*, 1675.
(17) Elger, G.; Kurreck, H.; Wiehe, A.; Johnen, E.; Fuhs, M.; Prisner, T.; Vrieze, J. *Acta Chem. Scand.* **1997**, *51* (5), 593.
(18) Wasielewski, M. R. *Chem. Rev.* **1992**, *92*, 435.
(19) Wiehe, A.; Senge, M. O.; Kurreck, H. *Liebigs Ann./Recueil* **1997**, 1051.
(20) Zimmermann, J.; von Gersdorff, J.; Kurreck, H.; Roder, B. T. *J. Photochem. Photobiol. B: Biol*. **1997**, *40*, 209.
(21) E-7 is a eutectic mixture of R_i-C_6H_5−C_6H_5−CN: $R_1 = C_5H_{11}$ (51%); $R_2 = C_7H_{15}$ (25%); $R_3 = C_8H_{17}O$ (16%); $R_4 = C_5H_{11}C_6H_5$ (8%).
(22) Regev, A.; Galili, T.; Levanon, H. *J. Chem. Phys*. **1991**, *95*, 7907.
(23) Gonen, O.; Levanon, H. *J. Chem. Phys.* **1986**, *84*, 4132.
(24) Regev, A.; Berman, A.; Levanon, H.; Murai, T.; Sessler, J. L. *Chem. Phys. Lett*. **1989**, *160*, 401.
(25) Levanon, H. *Rev. Chem. Intermed*. **1987**, *8*, 287.
(26) Gonen, O.; Levanon, H. *J. Phys. Chem.* **1985**, *89*, 1637.
(27) Clarke, R. H.; Connors, R. E. *Chem. Phys. Lett.* **1975**, *33*, 365.
(28) Marcus, R. A. *J. Chem. Phys*. **1956**, *24*, 966.
(29) Rips, I.; Jortner, J. *J. Chem. Phys*. **1987**, *87*, 2090.
(30) Schlüpmann, J.; Salikhov, K. M.; Plato, M.; Jaegermann, P.; Lendzian, F.; Möbius, K. *Appl. Magn. Reson*. **1991**, *2*, 117.
(31) Hales, B. J. *J. Am. Chem. Soc*. **1975**, *97*, 5993.
(32) Wasielewski, M. R.; Niemczyk, M. P. *J. Am. Chem. Soc.* **1984**, *106*, 5043.
(33) Levanon, H.; Norris, J. R. *Chem. Rev.* **1978**, *78*, 185.
(34) Bittl, R.; Treutlein, H.; Schulten, K. In *Springer Series in Chemical Physics, Antennas and Reaction Centers of Photosynthetic Bacteria*; Michel-Beyerle, M. E., Ed.; Springer: Berlin, 1985; Vol. 42, p 264.
(35) O'Malley, P. J.; Babcock, J. T. *J. Am. Chem. Soc*. **1986**, *108*, 3995.
(36) Lendzian, F.; von Maltzan, B. *Chem. Phys. Lett.* **1991**, *180*, 191.
(37) Schlüpmann, J.; Lendzian, F.; Plato, M.; Möbius, K. *J. Chem. Soc., Faraday Trans*. **1993**, *89*, 2853.
(38) Lendzian, F.; Schlüpmann, J.; von Gersdorff, J.; Möbius, K.; Kurreck, H. *Angew. Chem., Int. Ed. Engl.* **1991**, *30*, 1461.
(39) Batchelor, S. N.; Sun, L.; Möbius, K.; Kurreck, H. *Magn. Reson. Chem.* **1995**, *33*, S28.
(40) Dieks, H.; Senge, M. O.; Kirste, B.; Kurreck, H. *J. Org. Chem.* **1997**, *62*, 8666.